Factors influencing tissue cyst yield in a murine model of chronic toxoplasmosis

Cortni A. Troublefield[a^], Robert D. Murphy[a,b], Joy S. Miracle[a] , Ryan W. Donkin[a] and Anthony P. Sinai[a*]

[a]Department of Microbiology, Immunology and Molecular Genetics,
[b]Department of Molecular and Cellular Biochemistry,
University of Kentucky College of Medicine, Lexington, KY 40536, USA

^ Current Address: Emergency Department, Good Samaritan Hospital,
University of Kentucky Healthcare.

*Corresponding Author: sinai@uky.edu

Running Title: Factors affecting *T. gondii* tissue cyst yield

Abstract

Recent advances into the unique biology of Toxoplasma tissue cysts and the bradyzoites they house necessitates optimization of tissue cyst recovery from infected mouse brains. Here, we present data from 68 tissue cyst purifications of Type II ME49 tissue cysts in CBA/J mice performed over a period of two years. The effects if infecting with both tissue culture tachyzoites as well as *ex vivo* tissue cysts were assessed. Significant mortality was restricted to tachyzoite infections with female mice being more susceptible. Infection with tissue cysts was associated with both lower overall symptomology and mortality exhibiting no sex bias. Cumulatively, host sex did not impact overall tissue cyst yields, although, tachyzoite initiated infections generated significantly higher yields compared to tissue cyst-initiated infections. Notably, serial passage of tissue cysts was accompanied with a decreasing trend for subsequent cyst recovery. The time of tissue cyst harvest, a potential reflection of bradyzoite physiological state, had no significant impact on subsequent cyst yield at the selected time points. In aggregate, the data reveal the considerable heterogeneity associated with tissue cyst yield making the design of adequately powered experiments critical. This is particularly the case for drug studies where overall tissue cyst burden currently serves as the primary and often sole metric of efficacy, as the data presented here demonstrate that cyst recovery between preparations of untreated animals can mirror the reported effects of drug treatment.

45 **Introduction**

46 *Toxoplasma gondii* is an important opportunistic infection in the context of HIV-AIDS
47 and other immunosuppressive conditions (1, 2). Transmission of the parasite is
48 mediated by two distinct encysted forms, the oocysts, shed at the end of the sexual
49 cycle in the feces of the definitive feline host (3, 4) and the tissue cysts formed with the
50 establishment of the chronic infection in all vertebrate hosts (5). The tropism of tissue
51 cysts to the central nervous system and muscle provides a mechanism of transmission
52 in the act of carnivory (6, 7). Indeed, consumption of raw or undercooked meat
53 contaminated with tissue cysts serves as a primary mechanism for transmission to
54 humans contributing to *Toxoplasma gondii* being a significant agent of food-borne
55 infection (6-8).

56 Despite their central role in transmission, little is known about the basic biology of
57 the tissue cyst (5). What is known is that the tissue cyst represents a genetically clonal
58 though physiologically heterogenous community of slow growing bradyzoite forms of the
59 parasite (5). Bradyzoites were long viewed to be dormant forms, a position that was
60 challenged by our work demonstrating that tissue cysts derived from infected mouse
61 brains contain bradyzoites exhibiting metabolic activity including the capacity to
62 replicate by endodyogeny (9). This critical finding has triggered a renewed interest in
63 bradyzoite biology as it provides a window into potential drug treatment for a form that
64 remains refractory to currently approved drugs (10).

65 The development of new treatments targeting encysted bradyzoites will be
66 fundamentally dependent on efficient means to generate tissue cysts in vivo for further
67 functional analyses (10-13). Here we build on our earlier work (9, 14) to identify factors

68 influencing tissue cyst yields from infected brains in a murine model of experimental
69 toxoplasmosis. In seeking to optimize the parameters contributing to tissue cyst
70 recovery from the infected brain, we assess the effect of sex, infection source , the
71 consequence of serial passage of tissue cysts between mice, and the effect of the
72 relative time of harvest on subsequent cyst yield. Additionally, tissue cyst yields were
73 assessed based on the mean recovery per infected animal while also considering per
74 capita yields accounting for animals succumbing to infection prior to harvesting. This
75 latter category proved to represent a significant proportion of animals infected with
76 tissue culture derived tachyzoites.

77 The data presented herein indicate that tissue cyst yields are impacted by
78 multiple factors necessitating consideration particularly in the interpretation of outcomes
79 of drug studies. Drug efficacy is currently evaluated exclusively based on tissue cyst
80 recovery which has a sensitivity limited to under two orders of magnitude. Thus, even
81 the most effective experimental drugs which reduce recovery by between 80-90% (10-
82 13, 15, 16), fall within the range of cyst recovery in the absence of any drug treatment
83 (5, 9) (and data presented in this study). We therefore need to reassess overall
84 approaches to understanding the chronic infection and focus at the level of encysted
85 bradyzoites, appreciating the heterogeneity of activity within the tissue cyst.
86 Development of these methods, several of which are currently underway in our
87 laboratory will greatly benefit from the optimization of tissue cyst yield, considering the
88 factors investigated here and other factors that remain to be identified.
89
90

91 **Materials and Methods**

92 **Parasite Line**

93 All infections using both tachyzoites and *ex vivo* brain derived tissue cysts utilized a
94 derivative of Type II ME49 parasites with a deletion of the HXGPRT (TGME49_200320)
95 gene (17). This line was generated using CRISPR-CAS9 mediated deletion of the gene
96 (18, 19) followed by selection with 6-Thioxanthine (6TX) (17). Selection of the targeting
97 sgRNA sequences followed published sequences targeting this gene (20). Specifically
98 TgHXGRPT(Exon2, +strand): ATGGTCTCCACCAGTGCTCC; TgHXGPRT (Exon3, -
99 strand): GACAAAATCCTCCTCCCTGG and TgHXGPRT (Exon5, +strand):
100 CTTCTTCGAGCACTTGTCC were introduced into the pSAG1::CAS(-GFP::sgUPRT)
101 plasmid (18, 19) to generate 3 distinct mutagenesis plasmids that were co-transfected
102 into Type II ME49 parasites. Initial enrichment for transfected parasites was achieved
103 using flow cytometry (21) prior to selection with 6-TX at 80mg/ml in αMEM with 7%
104 dialyzed FBS. Following drug selection, cloning and confirmation of the mutation,
105 parasites were maintained by serial passage in HFF cells grown in bicarbonate buffered
106 αMEM supplemented with 7% heat inactivated FBS, 50mM glutamine and 25mM
107 Penicillin/Streptomycin at 37°C in 5% CO_2. This derivative exhibited identical growth
108 characteristics and *in vitro* switching in response to pH8.2/ambient CO_2 incubation to
109 wild type ME49 parasites obtained from the AIDS Resource Center (data not shown).
110

111 **Mouse infection model**

112 Both male and female CBA/J mice (strain #00065, The Jackson Laboratory, Bar Harbor
113 Maine) were used in these studies. Mice were procured at age 4-6 weeks and

114 habituated in the animal facility for a minimum of 1 week and were provided with
115 standard chow (Teklad 2918 irradiated 18%CP rodent diet, Envigo, Indianapolis, IN)
116 and water *ad libitum* during the course of these studies. Mice were infected with
117 Toxoplasma by intraperitoneal (i.p.) injection typically within 2.5 weeks of receipt from
118 the vendor. Infection with cell culture derived tachyzoites was performed using syringe
119 passaged parasites recovered in PBS and kept on ice. At least two independent counts
120 were used to establish the number of tachyzoites in the seed stock. Innocula containing
121 100 tachyzoites/ 200μl per mouse (500 tachyzoites/ml) diluted into serum free OptiMEM
122 (Gibco). The inoculating suspension was maintained on ice and 200μl injected i.p. per
123 mouse. Prior to injection mice were mildly anesthetized with 30% isoflurane in
124 propylene glycol using a drop jar method (22).

125 Infection of animals with brain derived tissue cysts was performed by diluting a
126 reserved volume of brain homogenate obtained in the course of purification of brain
127 derived tissue cysts. Brain homogenate corresponding to 20 cysts diluted to 200μl using
128 OptiMEM were used as the innoculum. Quantification of tissue cyst burdens within
129 brain homogenates was established as previously described below (14).

130 In this study, in addition to tracking the tissue cyst burden from tachyzoite
131 initiated (T) infection, we monitored the effect of serial passage of tissue cysts on the
132 overall tissue cyst burden. Accordingly, the first cycle of infection initiated from tissue
133 cysts (bradyzoites) generated from a tachyzoite-initiated infection represented the B1
134 inoculum. Subsequent serial passage of tissue cysts from B1 initiated infections were
135 designated B2, followed by B3 and B4 (Figure 1A,B).

136 Following infection, mice were monitored daily for the development of symptoms
137 with the monitoring increased to at least twice daily once animals became symptomatic.
138 The progression of the infection was monitored using a body score index rubric (Figure
139 1 C). Notably, this rubric, which reflects the typical progression of symptoms, does not
140 always follow the exact progression, but does provide a framework to standardize the
141 severity of symptoms based on physical observation. As symptoms progressed,
142 supportive treatment was limited to the provision of a gel-based diet (DietGel 76A, Clear
143 H_2O, Westbrook, Maine) and wet chow on the cage floor. Sub dermal saline injections
144 for animals presenting as dehydrated was provided as additional supportive. No
145 additional interventions were provided to symptomatic animals as the administration of
146 either anti-toxoplasma treatments or anti-inflammatory drugs would alter the
147 progression to the encysted state. All studies involving the use of animals and
148 biohazards were approved by the Institutional Animal Care and Use Committee
149 (IACUC) and Institutional Biosafety (IBC) Committees respectively at the University of
150 Kentucky.
151

152 **Tissue Cyst Purification and Quantification**

153 Tissue cyst purifications were performed using a modified Percoll gradient method (9,
154 14) based on the classic Cornelison protocol (23). Of note, all tissue cyst yields reported
155 in this work were generated from Percoll gradients loaded with the brain homogenates
156 from 2 brains of animals of the same sex. While mixed sex gradients were run, these
157 data are excluded from the current analysis. Additionally, tissue cysts recovered from
158 running single brain gradients using a modified protocol (14) are not reported here as

159 prior work has demonstrated that recovery of cysts from two brain gradients is optimal
160 with significantly lower yields when processing single brain gradients (14).
161 Quantification of cyst burdens was established by the summation of the relative cyst
162 numbers detected in Percoll fractions as previously described (9, 14). A mean yield per
163 mouse was calculated from the total yield of a Percoll gradient, resulting in a single data
164 point from a two-brain preparation.

165 Quantification of the distribution of tissue cysts within the Percoll gradients was
166 normalized relative to the location of the erythrocytes within the gradients, which was
167 assigned fraction 0. This permits the normalization of distribution of tissue cysts
168 accounting for potential variation in the establishment of the gradients.

169

170 **Statistical Analysis**

171 Mouse mortality for each sex following either tachyzoite-initiated or tissue cyst-
172 initiated infection was evaluated using a Kaplan-Meier estimator. Additionally, a
173 graphical representation of disease progression is based on body score index data
174 rubric over the first 28 days of infection was plotted as stacked graph.

175 The distribution of the data related to tissue cyst yield accumulated over the
176 course of this study was found to be non-parametric. We therefore performed statistical
177 analyses with both the raw data and following a logN- transformation (Ln-transform) of
178 the data. The former data are presented in the form of a scatter plot presenting all data
179 points while the Ln-transformed data are presented as box and whisker plots. All
180 statistical analyses were performed using GraphPad Prism with the specific tests
181 applied indicated within the figure legends.

182 **Results**

183 **Generation of a Type II ME49ΔHXGPRT line**

184 The generation of a Type II ME49DHXGPRT line for use in this study was
185 undertaken to establish the characteristics of what constitutes a parental (WT) line for
186 subsequent studies targeting specific genes that are ongoing and beyond the scope of
187 the current study. The targeted disruption of the hypoxanthine-xanthine guanine
188 phosphoribosyl transferase gene (TgME49_200320) has been demonstrated to have no
189 impact on growth both in culture and *in vivo* (acute infection) (17, 20, 24). Loss of
190 TgHXGPRT can be positively selected for using the subversive substrate 6-thioxanthine
191 (6-TX) (17, 24). Importantly, restoration of activity in ΔTgHXGPRT lines allows for
192 positive selection using a combination of mycophenolic acid and xanthine (MPA-X)
193 providing a marker for positive selection in subsequent gene targeting/ complementation
194 studies (Fig. 2A.) (17, 24).

195 To disrupt the HXGPRT locus in the prototypical cyst forming Type II ME49
196 parasites a shotgun CRISPR-Cas9 strategy (18, 19) was employed as described in the
197 materials and methods. Drug selected parasites were cloned by limiting dilution and the
198 disruption of the gene confirmed by PCR amplification of the locus and sequencing
199 across the mutation lesion (Figure. 2BC). Importantly infectivity and growth
200 characteristics assessed by both replication assays at 24 hours post infection and
201 plaque assays were identical to those of the parental WT ME49 line (data not shown).
202 In addition, the selected clonal TgME49ΔHXGPRT line exhibited identical rates of stage
203 conversion relative to wild type ME49 (data not shown). Finally, this line exhibits no
204 significant difference in the capacity to establish both an acute and chronic infection in

205 mice as detailed extensively below. For these reasons we designate the
206 TgME49ΔHXGPRT parasites, used exclusively in this study as wild type (WT).
207
208 **Differential effects of tachyzoite versus tissue cyst infections on mortality**
209 Reports in the literature and our prior experience reveal a considerable
210 heterogeneity in the mortality caused by ME49 tachyzoites during the course of the
211 acute infection (9, 25). These can range from LD_{50} values of 100 to 10^4 parasites (i.p.),
212 with enhanced virulence selected for by passage in culture. Acute virulence is
213 additionally impacted by mouse genetics which directly or indirectly affect the overall
214 cyst burden (26). In this regard, the CBA/J mouse presents an optimal balance of
215 survival during the acute infection and tissue cyst yields in the brain (9, 26). The
216 recovery of tissue cysts however is inherently highly variable (9, 25) and influenced by
217 a number of factors as discussed below.
218 In our earlier studies we used female mice exclusively and did not differentiate
219 between tachyzoite or tissue cyst-initiated infections (9). Here, we examined the effect
220 of sex as a variable, as well as the effect of the inoculum on overall survival during the
221 progression of the acute phase and entry into the early chronic phase (days 0-28).
222 Animals were monitored daily and at least twice daily once symptomatic. A body score
223 index, assessing both the physical condition of the animal and its level of activity, was
224 used to assess the progression of the infection (Fig. 1C). Infection with tachyzoites
225 resulted in significant mortality in mice of both sexes, with female mice exhibiting
226 significantly greater levels of mortality compared to males (Fig. 3A). Notably disease

227 progression following tachyzoite infection was rapid with fewer animals surviving despite
228 supportive treatment detailed in the materials and methods (Fig. 3B).
229 In contrast, relatively low mortality was observed for both sexes with tissue cyst (
230 initiated infections (Figure. 3C). This low incidence of mortality was mirrored by the low
231 overall symptomology as well as temporal delay in the onset of symptoms (Figure 3D).
232 This finding is meaningful in light of the fact that 20 tissue cysts likely possess in excess
233 of 10^5 parasites (9), a number at least 3 orders of magnitude greater than those causing
234 significant mortality with tachyzoite infections.
235
236 **Additional symptomology observed in *T. gondii* infected animals.**
237 While the disease progression rubric follows the course of symptomatic disease
238 and recovery during the acute phase and into the chronic infection (Fig. 1C), there were
239 additional adverse events that occurred both during the acute (weeks 1-3) and deep into
240 the chronic infection. The most prevalent of these was the development of a head tilt
241 resulting in animals leaning to one side, sometimes to the extent they exhibited difficulty
242 in lifting their head to feed or drink despite the fact that they often appeared as alert and
243 healthy (Fig. 4). The presentation of head tilts appeared spontaneously with mild head
244 tilts resolving or becoming moderate and severe. Affected animals tended to move in a
245 circular pattern in the direction of the head tilt (clockwise if tilted to the right and
246 counterclockwise when tilted to the left) and varying degrees of a loss of proprioception
247 (Supplemental Data 1). Supportive care was provided, however in most cases animals
248 exhibiting more severe head tilts needed to be euthanized due to their inability to
249 access food or water. During the studies reported here, head tilts (both resolving and

250 progressing) were observed in roughly 20% of animals suggesting they were being
251 triggered by the infection. Among these close to 12% presented with mild or moderate
252 head tilts (13.75% male and 6.25% female) that did not necessitate euthanasia, and 8%
253 (8.75% male and 6.25% female) of animals, with severe head tilts necessitating
254 euthanasia. Notably, there was no observable pattern among the cohorts of infected
255 mice correlating with the development of a head tilt that would be predictive in any way.
256 Consistent with emerging reports (27), infected mice presented with observed
257 seizures both during the acute and chronic phases of infection. In several instances
258 observed seizure were severe enough to warrant euthanasia. It is possible that
259 otherwise healthy looking infected animals that were found dead during the routine daily
260 inspections had succumbed to a seizure. Finally, we observed multiple instances of
261 penile prolapse in male animals which in several instances did not resolve resulting in
262 difficulty with urination and infections necessitating premature euthanasia. With recent
263 reports suggesting colonization of the rodent male genital tract in toxoplasma infections
264 (28, 29), it is conceivable that these symptoms may be connected indirectly with
265 infection.
266

267 **Effect of mouse sex and infection type on tissue cyst recovery**

268 The effect of a mouse's sex on the acute infection, its immune responses to that
269 infection, and other aspects of the chronic infection have been investigated (30-35).
270 Less has been done to establish if the sex of the host animal impacts the recovery of
271 tissue cysts for infections initiated with either tachyzoites or tissue cysts. While sex
272 based differences have been described (30-35), the overall recovery of tissue cysts

273 from infected from male vs female mice infected with either tachyzoites and tissue cysts
274 showed no difference (Fig. 5A,A'). We therefore examined how the inoculum type
275 affected the overall recovery of tissue cysts at multiple time points of harvest. The
276 results clearly indicate that tachyzoite initiated infections consistently generate higher
277 tissue cyst burdens than infections initiated with tissue cysts (Fig. 5B,B'). Of note the
278 lower number of tachyzoite-initiated cyst purifications meeting the criteria for inclusion (2
279 animals of the same sex- see materials and methods) was due to the high overall
280 mortality associated with tachyzoite infections that precluded an accurate quantification
281 of tissue cysts.
282

283 **Effect of serial tissue cyst passage on subsequent cyst yields.**

284 In light of the lower mortality associated with tissue cyst initiated infections we
285 examined whether serial passage of tissue cysts represented a potential means to
286 mitigate tachyzoite associated mortality (Fig. 6A,A'). The segregation of data based on
287 bradyzoite passage number (B1,B2, B3,B4) confirmed not only the lower cyst
288 recoveries compared to tachyzoite infections but also a trend of diminishing cyst yields.
289 (Fig. 6A,A'). In light of the trend of lower yields with passage, a limited analysis was
290 performed to assess the consequence of infection with cysts following 3 serial passages
291 though mice (B3). The resulting yield for B4 cysts in the low 100's, close to the level of
292 detection precluded further serial passages (Fig. 6A,A',B). Together these results
293 suggest that serial passage within CBA/J mice, while exhibiting low overall mortality
294 needs to be balanced with the diminishing yields as quantified on a per mouse infected
295 basis (Fig. 6B).

296 **Effect of time of harvest on subsequent tissue cyst burden**

297 Contrary to long standing dogma, the chronic infection is considerably more
298 dynamic than previously thought (5, 9). Our earlier work (5, 9) suggested that the
299 physical properties of tissue cysts varied, defined by the distribution of their density in
300 Percoll gradients at their times of harvest and is supported in the current data (Fig. 7).
301 These shifts may reflect cyclical changes in the physical properties of the tissue cysts
302 associated with patterns of replication hinted at by the dynamic nature of TgIMC3
303 (TgME49_244030) labeling, a marker for both active/recent replication (9, 36) and the
304 time since a specific bradyzoite last replicated (9). Such episodic events can result in
305 significant changes on the overall packing density, established by quantifying the actual
306 number of bradyzoites within tissue cysts thereby impacting their density in the
307 gradients (9).

308 TgIMC3 intensity is as a surrogate for the birth-dating of individual bradyzoites
309 that can serve as an indicator of active growth or relative dormancy (9). As such, the
310 proportion of “younger” and more active bradyzoites relative to their inactive peers
311 within the same tissue cyst can potentially impact their capacity to establish a
312 subsequent infections and thereby the overall cyst yield. We therefore reexamined the
313 data for both tachyzoite and bradyzoite-initiated infections resolving whether the time
314 tissue cysts were harvested affected the overall tissue cyst yield in the subsequent
315 infection cycle. What is clear is that while bradyzoite initiated infections as a whole
316 typically yield lower cyst recovery compared to tachyzoite (Fig. 5B,B’), the time of
317 harvest did not significantly impact the subsequent recovery of tissue cysts in
318 subsequent purifications (Fig 8A,A’). Interestingly, infection with tissue cysts recovered

319 at Week 4, a time point earlier in the chronic phase where active replication is projected
320 to be most pronounced (9), produced a large range of subsequent cyst yields. This
321 broad range however was not found to be statistically significant relative to Week 5
322 initiated cysts, when the lowest metabolic activity is expected (9) and Week 6 cysts
323 where activity is projected to be on an upward trajectory in the cycle (9). Interestingly,
324 tissue cyst yields following infections with B2 and B3 tissue cysts at all "ages" had no
325 impact on subsequent yield but trended lower than recovery following infection with B1
326 cysts (Fig. 6B).
327

328 **Discussion**

329 Bradyzoite within tissue cysts are arguably the most clinically relevant form in
330 reactivated disease upon immune suppression (10, 37, 38). Despite its central role in
331 the pathogenesis, little is known about the biology of the bradyzoite and the community
332 of bradyzoites that represent each individual tissue cyst (5). Notably, while bradyzoites
333 within a tissue cyst are genetically clonal, they represent a physiologically diverse
334 population that varies from cyst to cyst even within the same animal (5, 9). As such, a
335 bradyzoite retains a level of plasticity, permitting it to remain in this state, dedifferentiate
336 into a tachyzoite during recrudescence or enter the sexual cycle in the feline gut (39). It
337 is tempting to speculate that the heterogeneity inherent within the genetically clonal
338 tissue cyst is central to the survival of the organism.

339 The variable effect of infection in the murine model has been well documented
340 with both parasite effectors and host factors engaged in a complex interplay defining
341 susceptibility and resistance (26, 32, 38, 40-42). Beyond the inherent variability

342 observed with the cyst burden, differences with regard to parasite lines and mouse
343 backgrounds (26), and differences with regard to the sensitivity of approaches used to
344 quantify the cyst burden present vastly different numbers as summarized in a
345 comprehensive review on the topic (25). These differences with the lack of
346 standardization complicate comparisons across studies, which is becoming increasingly
347 important with the renewed focus on the chronic infection. In the context of cyst
348 formation and yield, the pairing of Type II ME49 parasites (and its derivatives, like the
349 ΔHXGPRT line used here) and CBA/J mice is recognized as providing the optimal
350 balance assuring reproducibly high tissue cyst yields (25). We have therefore used this
351 specific pairing but found in the course of the studies presented that establishing the
352 conditions for high tissue cyst yields is considerably more nuanced.
353 While there is no argument with regard to lethality of the mouse hypervirulent
354 Type I strains (RH, GT1), there is considerable variation in the observed LD_{50} values
355 dependent on the passage history of the parasite and the mouse background used in
356 infection (25). Indeed, *in vitro* passage of ME49 in tissue culture selects for mouse
357 hypervirulence resulting in a 2 order of magnitude or greater reduction in the LD_{50} value
358 (from $10e^4$ to 100 or fewer organisms) (26, 43, 44). This is observed to be the case with
359 the lab adapted ME49, and ME49ΔHXGPRT used here. Tachyzoite initiated infections
360 resulted in considerable mortality upon infection with 100 tachyzoites, with a statistically
361 different susceptibility profile for male vs female animals (Fig. 3A). As such, female mice
362 tended to get sicker earlier and succumb at higher rates relative to males in response to
363 i.p. injection with 100 ME49 tachyzoites during the acute infection (Fig. 3B). Recent
364 work from the Knoll laboratory examining the transcriptional responses within the host

365 during the progression of the chronic infection highlights clear differences between the
366 responses between the sexes (44), despite the overall response profile based on
367 several other criteria being fairly similar. Of note, similar to this study, they used CBA/J
368 mice (albeit of different ages than used here) of both sexes and Type II ME49 parasites
369 maintained in tissue culture. Yet, infection doses of 10^4 allowed for survival in the acute
370 phase and establishment of the chronic infection (44), highlighting the importance of
371 empirically establishing the specific tachyzoite infection regimen, as sex, the age of the
372 mice as well as additional factors impact the outcome of the acute infection that
373 precedes and is essential to the establishment of the chronic infection being
374 interrogated here.

375 In a previous study, using exclusively female mice, we established that infection
376 with 20 *ex-vivo* tissue cysts i.p. from infected brain homogenates reproducibly
377 generated robust cyst yields (9). Extending these findings we confirmed that infection
378 with tissue cysts of animals of both sexes is associated with very low mortality or
379 symptomology (Fig. 3C.D.). Despite the absence of overt symptoms during the course
380 of the infection, tissue cysts were recoverable from the brains of infected animals, of
381 both sexes with no sex bias related to yield (Fig. 5A,A'). Differences in overall yield were
382 observed when comparing tachyzoite initiated vs tissue cyst initiate infections (Fig. 5B).

383 One aspect of the toxoplasma infection, that has not been reported on
384 previously, is the development of a head tilt which in severe cases necessitates
385 euthanasia of the affected mouse (Fig. 4). Examination of available literature indicates
386 that infection-associated head tilts in mice have been noted with bacterial infections of
387 the inner ear (45, 46).

388 Direct brain/CNS involvement is noted in the case of a murine *Plasmodium*
389 *berghei* study where it may be linked to intra-cerebral hemorrhages (47). Cerebral
390 hemorrhages are also associated with increased rodent head tilts in an ischemia
391 reperfusion injury model, independent of an infection being present (48, 49). Finally,
392 dysregulation of inflammatory responses resulting in intracerebral inflammatory foci and
393 linked to interferon gamma signaling in a model for autoimmune encephalomyelitis is
394 also associated with increased incidence of a head tilt (50, 51). Further indication for an
395 association between an aberrant inflammatory response is evident from head-tilt mice
396 encoding specific mutation in Nox3, the NADPH oxidase involved in inflammation (52).
397 Finally, the absence of any reports regarding the development of head-tilts in the *T.*
398 *gondii* murine infection may further indicate differential susceptibility of different mouse
399 strains, whereby the CBA/J animals used here are predisposed to developing this
400 condition.

401 The recovery of tissue cysts following infection with either tachyzoites of
402 encysted bradyzoites exhibited no sex specific differences (Fig 5A,A') suggesting that
403 the differences seen following tachyzoite infection were likely due to differences in the
404 host response as opposed to factors intrinsic to the parasite. The more aggressive host
405 response in tachyzoites paradoxically resulted in significantly higher tissue cyst
406 recovery in surviving mice (Fig 3A,B and Fig 6B) compared to the cumulative recovery
407 following cyst infection where lower symptomology and mortality was observed (Fig.
408 3C,D and Fig. 6). This finding would suggest that maintenance of the infection by serial
409 passage of brain derived *ex vivo* tissue cysts would effectively get around the issue of
410 tachyzoite infection associated mortality which precludes cyst recovery. Unfortunately,

411 our data establish that serial passage of tissue cysts results in a progressive trend
412 toward reduction in overall recovery of cysts (Fig. 6). This indicates the need to re-
413 initiate an infection cycle with tachyzoites, despite high mortality, to sustain cyst
414 numbers for downstream analysis. The trend of decreasing cyst yields is not observed
415 in a ME49 line maintained in the Wilson laboratory by serial passage over multiple years
416 in mice (43). A key difference in that maintenance protocol is the “re-charging” of that
417 line in out bred Swiss Webster animals (43) wherein presumed epigenetic changes are
418 reinstituted to permit the restoration of high cyst yields upon return to infections in
419 inbred mice.

420 Our prior and ongoing analysis of bradyzoite replication within tissue cysts points
421 to largely asynchronous growth that broadly follows a cyclical pattern at least during the
422 first 8 weeks of infection (9). The inner membrane complex protein TgIMC3 (36) serves
423 as a reporter for both parasite birth-dating as well as their relative age based on the
424 intensity of labeling (9). Thus, early in the chronic phase, at week 3 post infection
425 (TgIMC3 high) parasites are in a higher state of metabolic activity associated with
426 extensive replication, both recent and active (9). At week 5 post infection this activity is
427 universally low (9), recovering to an intermediate level at week 8 (9). We reasoned
428 therefore that infection of mice with more “active’ cysts could result in overall higher cyst
429 yields. This however was not found to be the case (Fig. 8). Rather, for bradyzoite
430 initiated infections, the passage cycle (B1,B2,B3) (Fig. 6, 8) appeared to be a primary
431 determinant of subsequent cyst recovery suggesting that the apparent reprogramming
432 by continuous maintenance in a given mouse background (CBA/J in this case) is a key
433 determinant for tissue cyst initiated infections.

434 Insights into the physiology of bradyzoites is derived primarily from *in vitro*
435 studies using stress-induced stage conversion (53-56). These studies while important
436 in addressing the machinery of stage conversion do not provide meaningful insights into
437 the actual biology of bradyzoites *in vivo*. What limited studies reveal is that despite
438 being genetically clonal, individual tissue cysts exhibit considerable physiological
439 heterogeneity with regard to the resident bradyzoites (5, 9). Our development of
440 imaging based approaches to quantify bradyzoite numbers within *ex vivo* purified cysts
441 revealed the scope of heterogeneity (5, 9), a feature that is reinforced by ongoing
442 studies with the development of imaging based quantitative physiological readouts,
443 including quantification of, mitochondrial morphology and activity (57), amylopectin and
444 replication potential (Patwardhan and Sinai, unpublished). These tools are revealing
445 insights into bradyzoite physiology that will inform drug discovery and development
446 against this currently intractable life cycle stage.

447 A fundamental limitation in the evaluation of potential drugs effective in the
448 chronic infection is the fact that efficacy measured by the apparent reduction in cyst
449 burdens following treatment are presented in percentage terms (10, 12, 13, 15, 16, 58).
450 While this level of sensitivity represents the currently acceptable norm, they fail to
451 address the mechanistic basis for drug susceptibility or resistance. Initiating
452 investigation at the level of resident bradyzoites with an appreciation for their
453 heterogeneity will lead to more meaningful insights into the biology of the recalcitrant life
454 cycle stage.

455 Our findings that variations in cyst yield analogous to what is reported for drug
456 treatment (Fig. 5,6,8) is influenced by nature of the initial inoculum, passage and other

457 yet to be determined factors highlights the inefficiency and potential inaccuracy of using
458 the recovery of tissue cysts as the sole metric of drug effectiveness. These issues can
459 be compounded further when using solely the cyst burden to assign functional attributes
460 to mutations in mutant parasite lines (56, 59, 60). As with studies on drug efficacy, the
461 experimental design has to be sufficiently powered to account for the inherent variability
462 in cyst recovery with wild type or parental parasites. As the field continues to recognize
463 that tissue cysts and the bradyzoites they house are not dormant entities, directed
464 physiologic, metabolomic and transcriptomic studies which will depend on being able to
465 recover high cyst numbers for analysis will become increasingly critical. Our objective
466 in compiling the data in the current study is to highlight factors driving cyst yield all of
467 which are subject to further refinement. We hope this work will encourage further
468 studies in the field aimed at optimizing the recovery of tissue cysts to promote
469 meaningful in-depth studies into this critical and fascinating life cycle stage of the
470 parasite.
471

472 **Acknowledgements**

473 The authors would like to acknowledge the assistance of Dr. Heather Bush and
474 the Biostatistics, Epidemiology and Research Design (BERD) Core at the University of
475 Kentucky for guidance with the statistical analysis of these data. The authors wish to
476 thank the vivarium staff of the Department of Laboratory Animal Research for their
477 support and assistance during the course of these studies. We thank Dr. Aashutosh
478 Tripathi for his feedback regarding this manuscript. This work is supported by grants

479 from the US National Institutes of Health RO1AI145335 and R21 AI150631 awarded to
480 A.P.S..

481

482 **Figure Legends**

483 **Figure 1A. Schematic of the infection model** initiated with tissue culture derived
484 tachyzoites or tissue cysts harvested from infected mouse brains. Purified tissue cysts
485 were either used for serial passage in CBA/J mice, analyzed by immunofluorescence
486 microscopy (IFA) or used in other applications (purification of RNA for transcriptomic
487 studies). **B**. Sequential passage of tissue cysts derived from an initial tachyzoite (T)
488 infection to establish the 1st (B1), 2nd (B2), 3rd (B3) and 4th (B4) passage. Passages
489 were performed using cysts harvested in Weeks 4,5 or 6 post infection.
490 **C**. Color coded body score index based on symptomology associated with the
491 progression of the chronic infection used to stage disease progression.

492

493 **Figure 2A**. **Generation of the ME49ΔTgHXGPRT line**
494 Nucleotide scavenging pathway identifying the basis for the positive and negative
495 selection associated with HXGPRT (HX) KO parasites. Parasites expressing HXGPRT
496 are susceptible to 6-ThioXanthine (6-TX) but resistant to Mycophenolic Acid (MPA) +
497 Xanthine. In contrast ΔHXGPRT parasites are resistant to 6-TX and sensitive to MPA-
498 Xanthine. **B**. Schematic depicting the genomic locus encoding HXGPRT identifying the
499 location of the PAM sites targeted with specific CRISPR-Cas9 constructs. **C**. Schematic
500 of the genomic organization of the ΔHXGPRT locus with the sequence dendogram

501 confirming the fusion of exons 2 and 5 due to the deletion of the intervening introns and
502 exons resulting in the KO phenotype.
503
504 **Figure 3. Effect of mouse sex on progression through the acute infection and**
505 **establishment of the chronic infection**. **A.** Infection of male (blue, N= 56) and female
506 (pink, N= 44) mice with 100 tissue culture derived tachyzoites injected i.p. reveal female
507 mice are significantly more susceptible to infection noted by earlier and more extensive
508 mortality compared to infection of male mice. (Log-rank P value = 0.0031 (**)).
509 **B**. Progression of disease symptomology based on a color coded body score index
510 described in Figure 1C. **C**. Low overall mortality was observed following infection of both
511 male (blue, N=63) or female (pink, N=56) mice with 20 *ex vivo* tissue cysts in brain
512 homogenate. The differences in mortality between male and female mice was not
513 statistically significant. **D**. Low mortality was associated with overall low symptomology
514 scored using a body score index in Figure 1C.
515
516 **Figure 4. Spectrum of head-tilt presentations in *Toxoplasma* infected mice**. A
517 mild head tilt which either spontaneously resolves or progresses to moderate head tilt to
518 a severe head tilt phenotype affecting motility, proprioception and balance. Video
519 recording of motility by head tilt presenting animals is provided in the Supplemental
520 Data.
521
522 **Figure 5A. Mouse sex does not impact overall tissue cyst recovery** based on yields
523 from both male (38 preps) and female (29 preps) mice infected by either tachyzoites or

524 tissue cysts. **A'.** In light of the non parametric distribution of the data statistical analysis
525 was performed on logN -transformed data. These analyses confirm the absence of any
526 statistically relevant differences in tissue cyst recovery as a result of mouse sex. **B.**
527 Tissue cyst recovery as a function of infection with tissue culture derived tachyzoites
528 (Tachy) compared to tissue cysts (Cyst) exposes a significant difference in cyst
529 recovery (Unpaired t test, 2 tailed: P value < 0.0001, ****). **B'.** Analysis of logN
530 transformed data confirms the significant differences in cyst yields between tachyzoite
531 and cyst initiated infections (Unpaired t test, 2 tailed: P value= 0.0001, ***).
532
533 **Figure 6. Tissue cyst recovery following serial passage of ex vivo tissue cysts**
534 **reveals a pattern of diminishing returns**. **A**. Segregation of cyst yield data from all
535 tissue cyst initiated infections based in passage number confirms the differences in cyst
536 yield are modest between tachyzoite (T) and the first tissue cyst cycle (B1) (One way
537 ANOVA Tukey's multiple comparisons test P value= 0.035, *). Significant differences
538 are found between tachyzoite (T) and the second (B2) (One way ANOVA Tukey's
539 multiple comparisons test P value < 0.0001, ****) and third (B3) (P value = 0.0003, ***)
540 cycles. The single data point for B4 precludes statistical analysis. There was not
541 statistical difference (ns) among the bradyzoite initiated infections (B1, B2, B3, B4). **A'**
542 LogN transformed data reveals no statistical difference between tachyzoite-initiated and
543 B1 cyst initiated infections on subsequent yield. Significant differences in cyst yield were
544 observed when comparing tachyzoite initiated infections with second (One way ANOVA
545 with Tukey's multiple comparison test P value = 0.0002, ***) and third cycle (B3) cyst
546 infections (P value = 0.0002, ***). Additionally, statistically significant differences were

547 noted between B1 and B3 initiated infections (P value= 0.036, *). **B**. Table indicating the
548 actual recovery of tissue cysts as a function of total animals infected based on infection
549 (Tachyzoite (T) vs cyst (B1, B2, B3, B4). Each prep included uses 2 mice of the same
550 sex. Specific details regarding inclusion criteria are described in the text.
551
552 **Figure 7. The physical characteristics of tissue cysts as a function of the time of**
553 **harvest** post infection reveal a dynamic distribution in Percoll gradients. The mean
554 distribution for the proportion of tissue cysts detected in individual fractions were plotted
555 for each time point (Week 3 n=10, Week 4 n= 23, Week 5 n=13, Week 6 m=13, Week
556 n=9, Week 8 n= 4). The gray shading in the graphs defines the fraction(s) within which
557 the median cyst distributions were recorded. Gradient fractions at the interface of the
558 90% and 40% Percoll steps representing the fraction concentrated in mouse RBC
559 served as Fraction 0. Tissue cyst distribution in the roughly 1ml fractions (collected a
560 from the 40% step through the brain homogenate overlaid on the 20% Percoll step were
561 plotted as percentage of the total recovered cysts.
562
563 **Figure 8.**
564 **A**. **Infection with tissue cysts harvested at Weeks 4, 5 and 6** along with the specific
565 serial passage number (B1, B2, B3, B4) exhibit no differences in sub-subsequent cyst
566 yields despite marked differences in their distributions within Percoll gradients. **A'** LogN
567 transformed data confirms the lack of differences in subsequent cyst recovery as a
568 function of the time of harvest of the infecting tissue cysts.
569

570 **Supplemental Data 1:**

571 **SD1: Video: Presentation of mild, moderate and severe head-tilt in *T. gondii***

572 **infected mice:**

573

574

575

576 **Literature Cited**

577 1. Dubey JP, Jones JL. 2008. Toxoplasma gondii infection in humans and animals in the United
578 States. Int J Parasitol 38:1257-78.
579 2. Wang ZD, Wang SC, Liu HH, Ma HY, Li ZY, Wei F, Zhu XQ, Liu Q. 2017. Prevalence and burden of
580 Toxoplasma gondii infection in HIV-infected people: a systematic review and meta-analysis.
581 Lancet HIV 4:e177-e188.
582 3. Alvarez Garcia G, Davidson R, Jokelainen P, Klevar S, Spano F, Seeber F. 2021. Identification of
583 Oocyst-Driven Toxoplasma gondii Infections in Humans and Animals through Stage-Specific
584 Serology-Current Status and Future Perspectives. Microorganisms 9.
585 4. Zhu S, Shapiro K, VanWormer E. 2022. Dynamics and epidemiology of Toxoplasma gondii oocyst
586 shedding in domestic and wild felids. Transbound Emerg Dis 69:2412-2423.
587 5. Sinai AP, Watts EA, Dhara A, Murphy RD, Gentry MS, Patwardhan A. 2016. Reexamining Chronic
588 Toxoplasma gondii Infection: Surprising Activity for a "Dormant" Parasite. Curr Clin Microbiol
589 Rep 3:175-185.
590 6. Dubey JP. 2009. History of the discovery of the life cycle of Toxoplasma gondii. Int J Parasitol
591 39:877-82.
592 7. Jones JL, Dubey JP. 2012. Foodborne toxoplasmosis. Clin Infect Dis 55:845-51.
593 8. Scallan E, Hoekstra RM, Mahon BE, Jones TF, Griffin PM. 2015. An assessment of the human
594 health impact of seven leading foodborne pathogens in the United States using disability
595 adjusted life years. Epidemiol Infect 143:2795-804.
596 9. Watts E, Zhao Y, Dhara A, Eller B, Patwardhan A, Sinai AP. 2015. Novel Approaches Reveal that
597 Toxoplasma gondii Bradyzoites within Tissue Cysts Are Dynamic and Replicating Entities In Vivo.
598 MBio 6:e01155-15.
599 10. Alday PH, Doggett JS. 2017. Drugs in development for toxoplasmosis: advances, challenges, and
600 current status. Drug Des Devel Ther 11:273-293.
601 11. Doggett JS, Nilsen A, Forquer I, Wegmann KW, Jones-Brando L, Yolken RH, Bordon C, Charman
602 SA, Katneni K, Schultz T, Burrows JN, Hinrichs DJ, Meunier B, Carruthers VB, Riscoe MK. 2012.
603 Endochin-like quinolones are highly efficacious against acute and latent experimental
604 toxoplasmosis. Proc Natl Acad Sci U S A 109:15936-41.
605 12. McPhillie M, Zhou Y, El Bissati K, Dubey J, Lorenzi H, Capper M, Lukens AK, Hickman M, Muench
606 S, Verma SK, Weber CR, Wheeler K, Gordon J, Sanders J, Moulton H, Wang K, Kim TK, He Y,
607 Santos T, Woods S, Lee P, Donkin D, Kim E, Fraczek L, Lykins J, Esaa F, Alibana-Clouser F, Dovgin
608 S, Weiss L, Brasseur G, Wirth D, Kent M, Hood L, Meunieur B, Roberts CW, Hasnain SS, Antonyuk
609 SV, Fishwick C, McLeod R. 2016. New paradigms for understanding and step changes in treating
610 active and chronic, persistent apicomplexan infections. Sci Rep 6:29179.
611 13. McPhillie MJ, Zhou Y, Hickman MR, Gordon JA, Weber CR, Li Q, Lee PJ, Amporndanai K, Johnson
612 RM, Darby H, Woods S, Li ZH, Priestley RS, Ristroph KD, Biering SB, El Bissati K, Hwang S, Hakim
613 FE, Dovgin SM, Lykins JD, Roberts L, Hargrave K, Cong H, Sinai AP, Muench SP, Dubey JP,
614 Prud'homme RK, Lorenzi HA, Biagini GA, Moreno SN, Roberts CW, Antonyuk SV, Fishwick CWG,
615 McLeod R. 2020. Potent Tetrahydroquinolone Eliminates Apicomplexan Parasites. Front Cell
616 Infect Microbiol 10:203.
617 14. Watts EA, Dhara A, Sinai AP. 2017. Purification Toxoplasma gondii Tissue Cysts Using Percoll
618 Gradients. Curr Protoc Microbiol 45:20C 2 1-20C 2 19.
619 15. Martynowicz J, Doggett JS, Sullivan WJ, Jr. 2020. Efficacy of Guanabenz Combination Therapy
620 against Chronic Toxoplasmosis across Multiple Mouse Strains. Antimicrob Agents Chemother 64.
621 16. Vidadala RS, Rivas KL, Ojo KK, Hulverson MA, Zambriski JA, Bruzual I, Schultz TL, Huang W, Zhang
622 Z, Scheele S, DeRocher AE, Choi R, Barrett LK, Siddaramaiah LK, Hol WG, Fan E, Merritt EA,

623 Parsons M, Freiberg G, Marsh K, Kempf DJ, Carruthers VB, Isoherranen N, Doggett JS, Van
624 Voorhis WC, Maly DJ. 2016. Development of an Orally Available and Central Nervous System
625 (CNS) Penetrant Toxoplasma gondii Calcium-Dependent Protein Kinase 1 (TgCDPK1) Inhibitor
626 with Minimal Human Ether-a-go-go-Related Gene (hERG) Activity for the Treatment of
627 Toxoplasmosis. J Med Chem 59:6531-46.
628 17. Donald RG, Roos DS. 1998. Gene knock-outs and allelic replacements in Toxoplasma gondii:
629 HXGPRT as a selectable marker for hit-and-run mutagenesis. Mol Biochem Parasitol 91:295-305.
630 18. Shen B, Brown K, Long S, Sibley LD. 2017. Development of CRISPR/Cas9 for Efficient Genome
631 Editing in Toxoplasma gondii. Methods Mol Biol 1498:79-103.
632 19. Shen B, Brown KM, Lee TD, Sibley LD. 2014. Efficient gene disruption in diverse strains of
633 Toxoplasma gondii using CRISPR/CAS9. mBio 5:e01114-14.
634 20. Sidik SM, Huet D, Ganesan SM, Huynh MH, Wang T, Nasamu AS, Thiru P, Saeij JP, Carruthers VB,
635 Niles JC, Lourido S. 2016. A Genome-wide CRISPR Screen in Toxoplasma Identifies Essential
636 Apicomplexan Genes. Cell 166:1423-1435 e12.
637 21. Dhara A, de Paula Baptista R, Kissinger JC, Snow EC, Sinai AP. 2017. Ablation of an Ovarian
638 Tumor Family Deubiquitinase Exposes the Underlying Regulation Governing the Plasticity of Cell
639 Cycle Progression in Toxoplasma gondii. mBio 8.
640 22. Nagate T, Chino T, Nishiyama C, Okuhara D, Tahara T, Maruyama Y, Kasahara H, Takashima K,
641 Kobayashi S, Motokawa Y, Muto S, Kuroda J. 2007. Diluted isoflurane as a suitable alternative for
642 diethyl ether for rat anaesthesia in regular toxicology studies. J Vet Med Sci 69:1137-43.
643 23. Cornelissen AW, Overdulve JP, Hoenderboom JM. 1981. Separation of Isospora (Toxoplasma)
644 gondii cysts and cystozoites from mouse brain tissue by continuous density-gradient
645 centrifugation. Parasitology 83:103-8.
646 24. Donald RG, Carter D, Ullman B, Roos DS. 1996. Insertional tagging, cloning, and expression of the
647 Toxoplasma gondii hypoxanthine-xanthine-guanine phosphoribosyltransferase gene. Use as a
648 selectable marker for stable transformation. J Biol Chem 271:14010-9.
649 25. Watson GF, Davis PH. 2019. Systematic review and meta-analysis of variation in Toxoplasma
650 gondii cyst burden in the murine model. Exp Parasitol 196:55-62.
651 26. Dubey JP. 1998. Comparative infectivity of Toxoplasma gondii bradyzoites in rats and mice. J
652 Parasitol 84:1279-82.
653 27. Glausen TG, Carrillo GL, Jin RM, Boyle JP, Saeij JPJ, Wohlfert EA, Fox MA, Blader IJ. 2021. The
654 Toxoplasma Polymorphic Effector GRA15 Mediates Seizure Induction by Modulating Interleukin-
655 1 Signaling in the Brain. mBio 12:e0133121.
656 28. Colinot DL, Garbuz T, Bosland MC, Wang L, Rice SE, Sullivan WJ, Jr., Arrizabalaga G, Jerde TJ.
657 2017. The common parasite Toxoplasma gondii induces prostatic inflammation and
658 microglandular hyperplasia in a mouse model. Prostate 77:1066-1075.
659 29. Crespillo-Andujar C, Diaz-Menendez M, Mora-Rillo M. 2018. Evidence for Previously Unidentified
660 Sexual Transmission of Protozoan Parasites. Emerg Infect Dis 24:602-603.
661 30. Alonaizan R, Woods S, Hargrave KE, Roberts CW. 2021. An Exaggerated Immune Response in
662 Female BALB/c Mice Controls Initial Toxoplasma gondii Multiplication but Increases Mortality
663 and Morbidity Relative to Male Mice. Pathogens 10.
664 31. Gatkowska J, Wieczorek M, Dziadek B, Dzitko K, Dlugonska H. 2013. Sex-dependent
665 neurotransmitter level changes in brains of Toxoplasma gondii infected mice. Exp Parasitol
666 133:1-7.
667 32. Kankova S, Holan V, Zajicova A, Kodym P, Flegr J. 2010. Modulation of immunity in mice with
668 latent toxoplasmosis--the experimental support for the immunosuppression hypothesis of
669 Toxoplasma-induced changes in reproduction of mice and humans. Parasitol Res 107:1421-7.

670 33. Li YE, Kannan G, Pletnikov MV, Yolken RH, Xiao J. 2015. Chronic infection of Toxoplasma gondii
671 downregulates miR-132 expression in multiple brain regions in a sex-dependent manner.
672 Parasitology 142:623-32.
673 34. Roberts CW, Cruickshank SM, Alexander J. 1995. Sex-determined resistance to Toxoplasma
674 gondii is associated with temporal differences in cytokine production. Infect Immun 63:2549-55.
675 35. Xiao J, Kannan G, Jones-Brando L, Brannock C, Krasnova IN, Cadet JL, Pletnikov M, Yolken RH.
676 2012. Sex-specific changes in gene expression and behavior induced by chronic Toxoplasma
677 infection in mice. Neuroscience 206:39-48.
678 36. Anderson-White BR, Ivey FD, Cheng K, Szatanek T, Lorestani A, Beckers CJ, Ferguson DJ, Sahoo
679 N, Gubbels MJ. 2011. A family of intermediate filament-like proteins is sequentially assembled
680 into the cytoskeleton of Toxoplasma gondii. Cellular microbiology 13:18-31.
681 37. Pereira-Chioccola VL, Vidal JE, Su C. 2009. Toxoplasma gondii infection and cerebral
682 toxoplasmosis in HIV-infected patients. Future Microbiol 4:1363-79.
683 38. Vidal JE. 2019. HIV-Related Cerebral Toxoplasmosis Revisited: Current Concepts and
684 Controversies of an Old Disease. J Int Assoc Provid AIDS Care 18:2325958219867315.
685 39. Sinai AP, Suvorova ES. 2020. The RESTRICTION checkpoint: a window of opportunity governing
686 developmental transitions in Toxoplasma gondii. Curr Opin Microbiol 58:99-105.
687 40. Berenreiterova M, Flegr J, Kubena AA, Nemec P. 2011. The distribution of Toxoplasma gondii
688 cysts in the brain of a mouse with latent toxoplasmosis: implications for the behavioral
689 manipulation hypothesis. PLoS One 6:e28925.
690 41. Brinkmann V, Remington JS, Sharma SD. 1987. Protective immunity in toxoplasmosis: correlation
691 between antibody response, brain cyst formation, T-cell activation, and survival in normal and B-
692 cell-deficient mice bearing the H-2k haplotype. Infect Immun 55:990-4.
693 42. Saeij JP, Boyle JP, Coller S, Taylor S, Sibley LD, Brooke-Powell ET, Ajioka JW, Boothroyd JC. 2006.
694 Polymorphic secreted kinases are key virulence factors in toxoplasmosis. Science 314:1780-3.
695 43. Goerner AL, Vizcarra EA, Hong DD, Bergersen KV, Alvarez CA, Talavera MA, Wilson EH, White
696 MW. 2020. An ex vivo model of Toxoplasma recrudescence. bioRxiv
697 doi:10.1101/2020.05.18.101931:2020.05.18.101931.
698 44. Garfoot AL, Cervantes PW, Knoll LJ. 2019. Transcriptional Analysis Shows a Robust Host
699 Response to Toxoplasma gondii during Early and Late Chronic Infection in Both Male and Female
700 Mice. Infect Immun 87.
701 45. Floyd R, Michel AO, Piersigilli A, Aronowitz E, Voss HU, Ricart Arbona RJ. 2021. Ethmoidal
702 meningoencephalocele in a C57BL/6J mouse. Lab Anim 55:181-188.
703 46. Collymore C, Giuliano F, Banks EK. 2019. Head Tilt in Immunodeficient Mice Due to
704 Contamination of Drinking Water by Burkholderia gladioli. J Am Assoc Lab Anim Sci 58:246-250.
705 47. Recuenco FC, Takano R, Chiba S, Sugi T, Takemae H, Murakoshi F, Ishiwa A, Inomata A, Horimoto
706 T, Kobayashi Y, Horiuchi N, Kato K. 2014. Lambda-carrageenan treatment exacerbates the
707 severity of cerebral malaria caused by Plasmodium berghei ANKA in BALB/c mice. Malar J
708 13:487.
709 48. Southard T, Brayton CF. 2011. Spontaneous unilateral brainstem infarction in Swiss mice. Vet
710 Pathol 48:726-9.
711 49. Van der Donckt C, Van Herck JL, Schrijvers DM, Vanhoutte G, Verhoye M, Blockx I, Van Der
712 Linden A, Bauters D, Lijnen HR, Sluimer JC, Roth L, Van Hove CE, Fransen P, Knaapen MW,
713 Hervent AS, De Keulenaer GW, Bult H, Martinet W, Herman AG, De Meyer GR. 2015. Elastin
714 fragmentation in atherosclerotic mice leads to intraplaque neovascularization, plaque rupture,
715 myocardial infarction, stroke, and sudden death. Eur Heart J 36:1049-58.

716 50. Lee E, Chanamara S, Pleasure D, Soulika AM. 2012. IFN-gamma signaling in the central nervous
717 system controls the course of experimental autoimmune encephalomyelitis independently of
718 the localization and composition of inflammatory foci. J Neuroinflammation 9:7.
719 51. Wensky AK, Furtado GC, Marcondes MC, Chen S, Manfra D, Lira SA, Zagzag D, Lafaille JJ. 2005.
720 IFN-gamma determines distinct clinical outcomes in autoimmune encephalomyelitis. J Immunol
721 174:1416-23.
722 52. Paffenholz R, Bergstrom RA, Pasutto F, Wabnitz P, Munroe RJ, Jagla W, Heinzmann U,
723 Marquardt A, Bareiss A, Laufs J, Russ A, Stumm G, Schimenti JC, Bergstrom DE. 2004. Vestibular
724 defects in head-tilt mice result from mutations in Nox3, encoding an NADPH oxidase. Genes Dev
725 18:486-91.
726 53. Sullivan WJ, Jr., Jeffers V. 2012. Mechanisms of Toxoplasma gondii persistence and latency.
727 FEMS Microbiol Rev 36:717-33.
728 54. Krishnan A, Kloehn J, Lunghi M, Chiappino-Pepe A, Waldman BS, Nicolas D, Varesio E, Hehl A,
729 Lourido S, Hatzimanikatis V, Soldati-Favre D. 2020. Functional and Computational Genomics
730 Reveal Unprecedented Flexibility in Stage-Specific Toxoplasma Metabolism. Cell Host Microbe
731 27:290-306 e11.
732 55. Bohne W, Heesemann J, Gross U. 1994. Reduced replication of Toxoplasma gondii is necessary
733 for induction of bradyzoite-specific antigens: a possible role for nitric oxide in triggering stage
734 conversion. Infect Immun 62:1761-7.
735 56. Waldman BS, Schwarz D, Wadsworth MH, 2nd, Saeij JP, Shalek AK, Lourido S. 2020.
736 Identification of a Master Regulator of Differentiation in Toxoplasma. Cell 180:359-372 e16.
737 57. Place BC, Troublefield C, Murphy RD, Sinai AP, Patwardhan A. 2021. Computer Aided Image
738 Processing to Facilitate Determination of Congruence in Manual Classification of Mitochondrial
739 Morphologies in Toxoplasma gondii Tissue Cysts. Annu Int Conf IEEE Eng Med Biol Soc
740 2021:3509-3513.
741 58. Doggett JS, Schultz T, Miller AJ, Bruzual I, Pou S, Winter R, Dodean R, Zakharov LN, Nilsen A,
742 Riscoe MK, Carruthers VB. 2020. Orally Bioavailable Endochin-Like Quinolone Carbonate Ester
743 Prodrug Reduces Toxoplasma gondii Brain Cysts. Antimicrob Agents Chemother 64.
744 59. Uboldi AD, McCoy JM, Blume M, Gerlic M, Ferguson DJ, Dagley LF, Beahan CT, Stapleton DI,
745 Gooley PR, Bacic A, Masters SL, Webb AI, McConville MJ, Tonkin CJ. 2015. Regulation of Starch
746 Stores by a Ca(2+)-Dependent Protein Kinase Is Essential for Viable Cyst Development in
747 Toxoplasma gondii. Cell Host Microbe 18:670-81.
748 60. Radke JB, Lucas O, De Silva EK, Ma Y, Sullivan WJ, Jr., Weiss LM, Llinas M, White MW. 2013.
749 ApiAP2 transcription factor restricts development of the Toxoplasma tissue cyst. Proc Natl Acad
750 Sci U S A 110:6871-6.
751

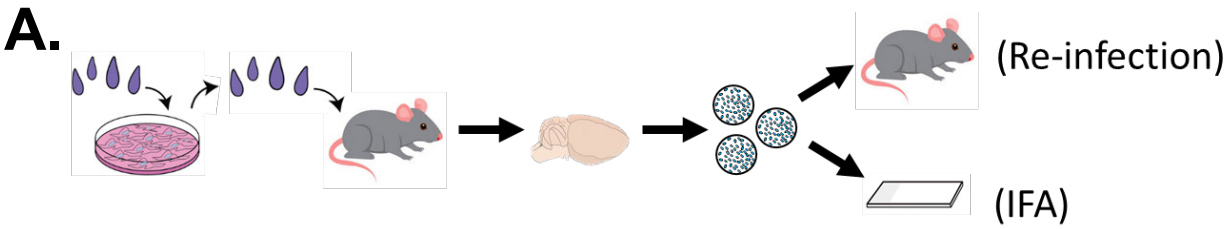

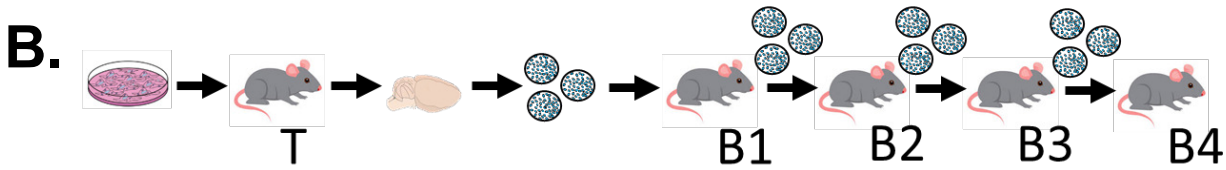

C.

		Ruffled Fur	Slight decrease in activity	Bilateral eye squinting	Shallow breathing	Hunched	Dehydrated	Marked decrease in activity	Inactive/no movement when prompted	Agonal breathing	Found deceased
Healthy	Stage 0										
Progression of acute illness	Stage 1	X	X								
	Stage 2	X	X	X	X						
	Stage 3	X	X	X	X	X	X	X			
Moribund/ deceased	Stage 4	X	X	X	X	X	X	X	X	X	X

Troublefield et al. 2022 **Figure 1**

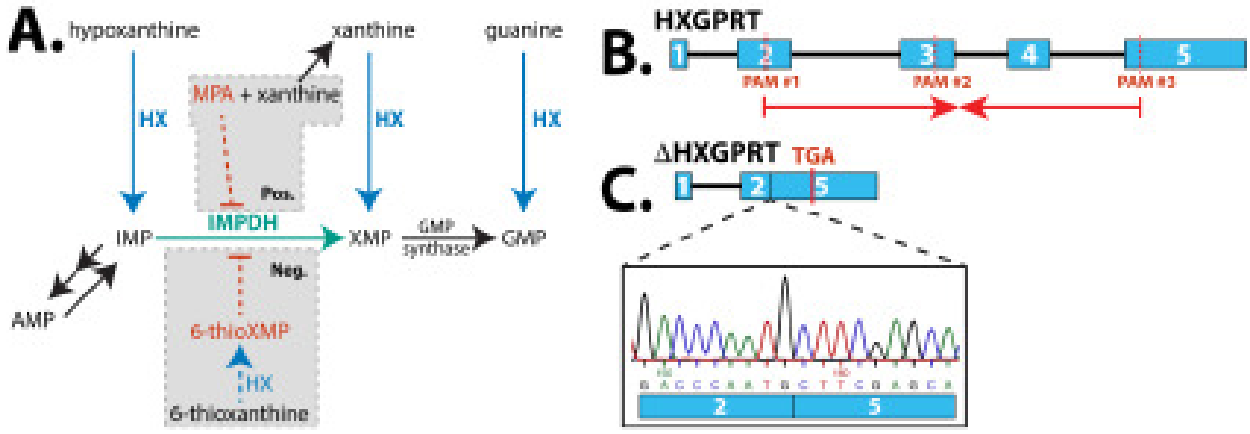

Troublefield et al. 2022 **Figure 2**

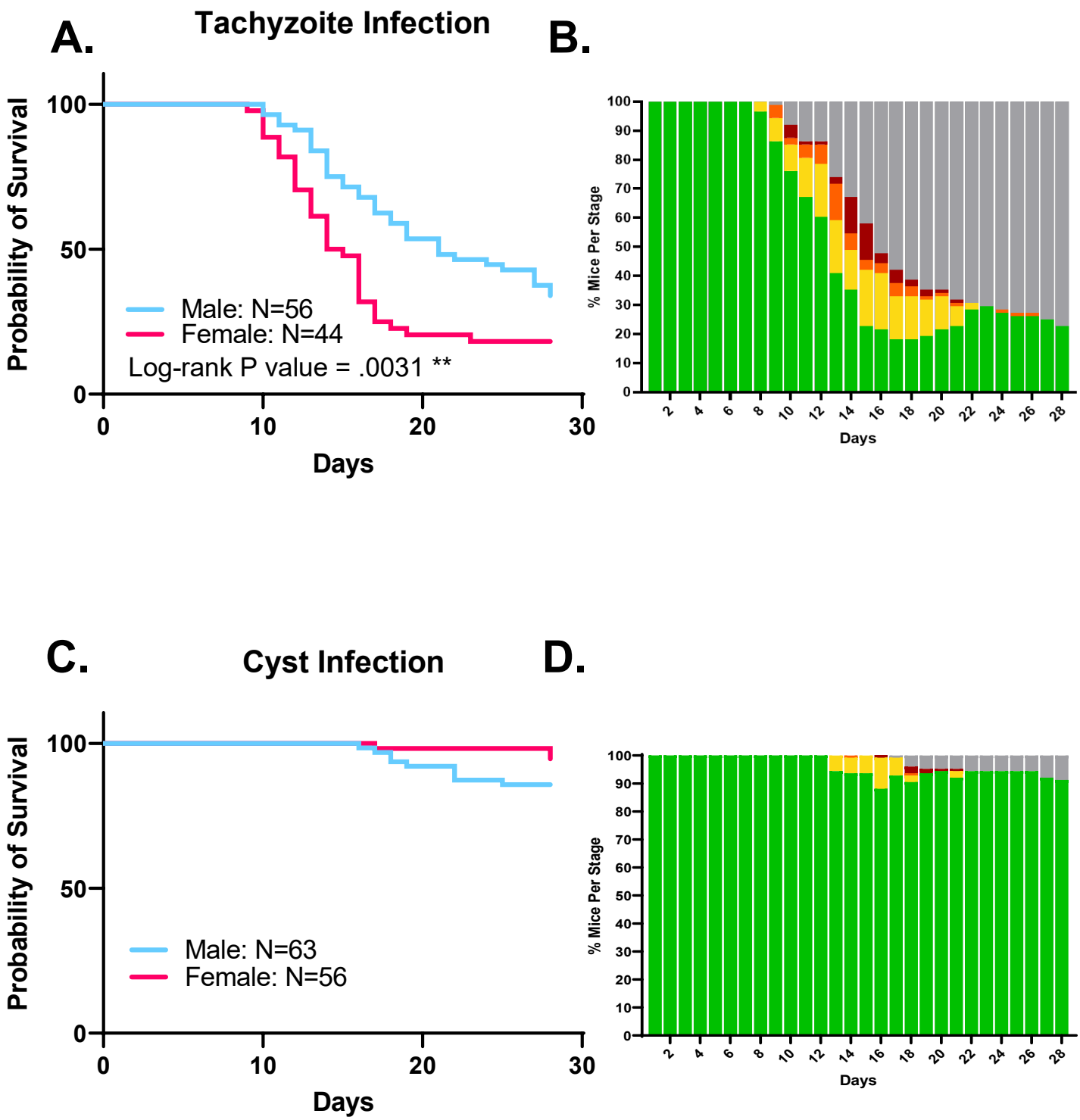

Troublefield et al. 2022 **Figure 3**

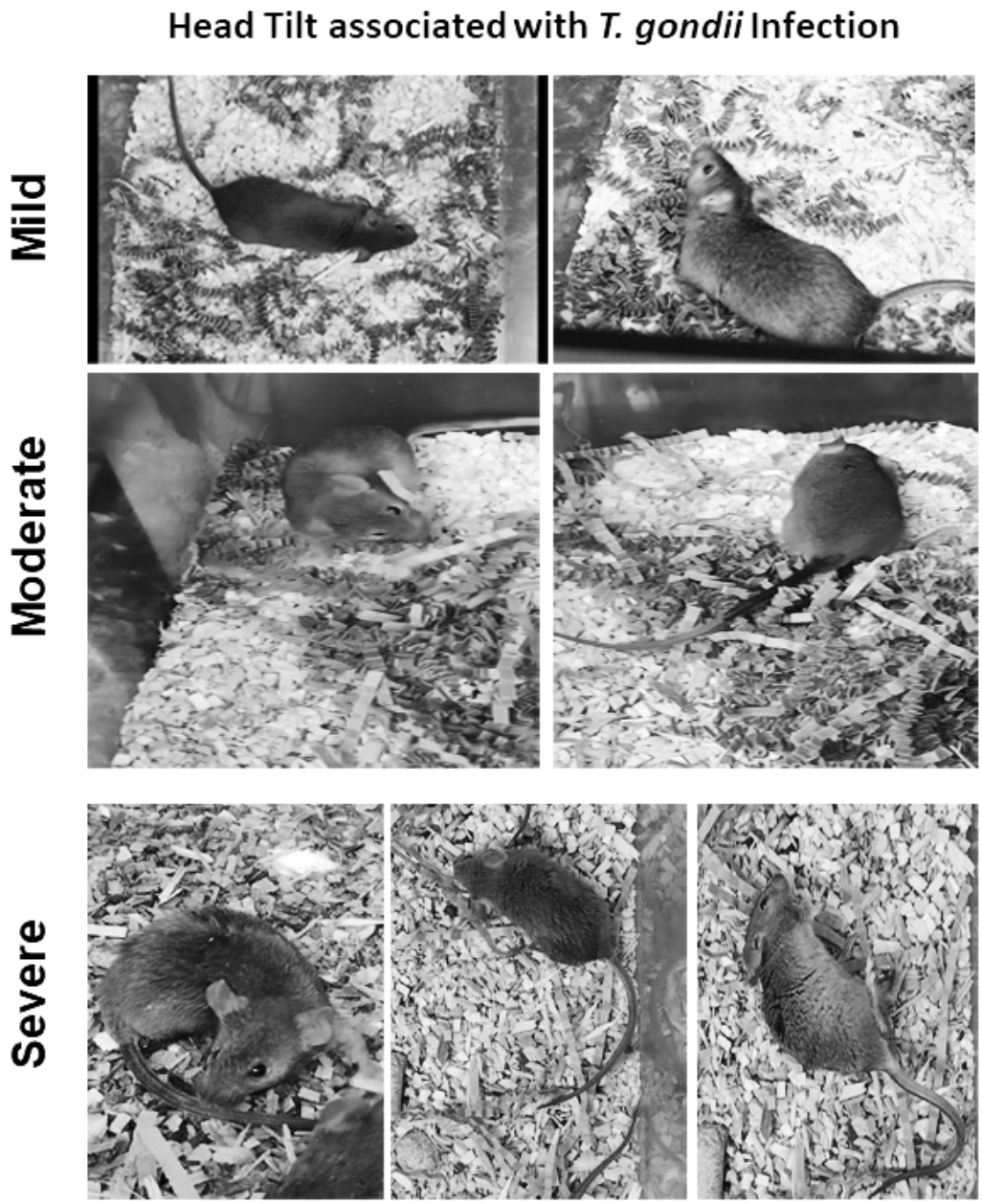

Troublefield et al. 2022 **Figure 4**

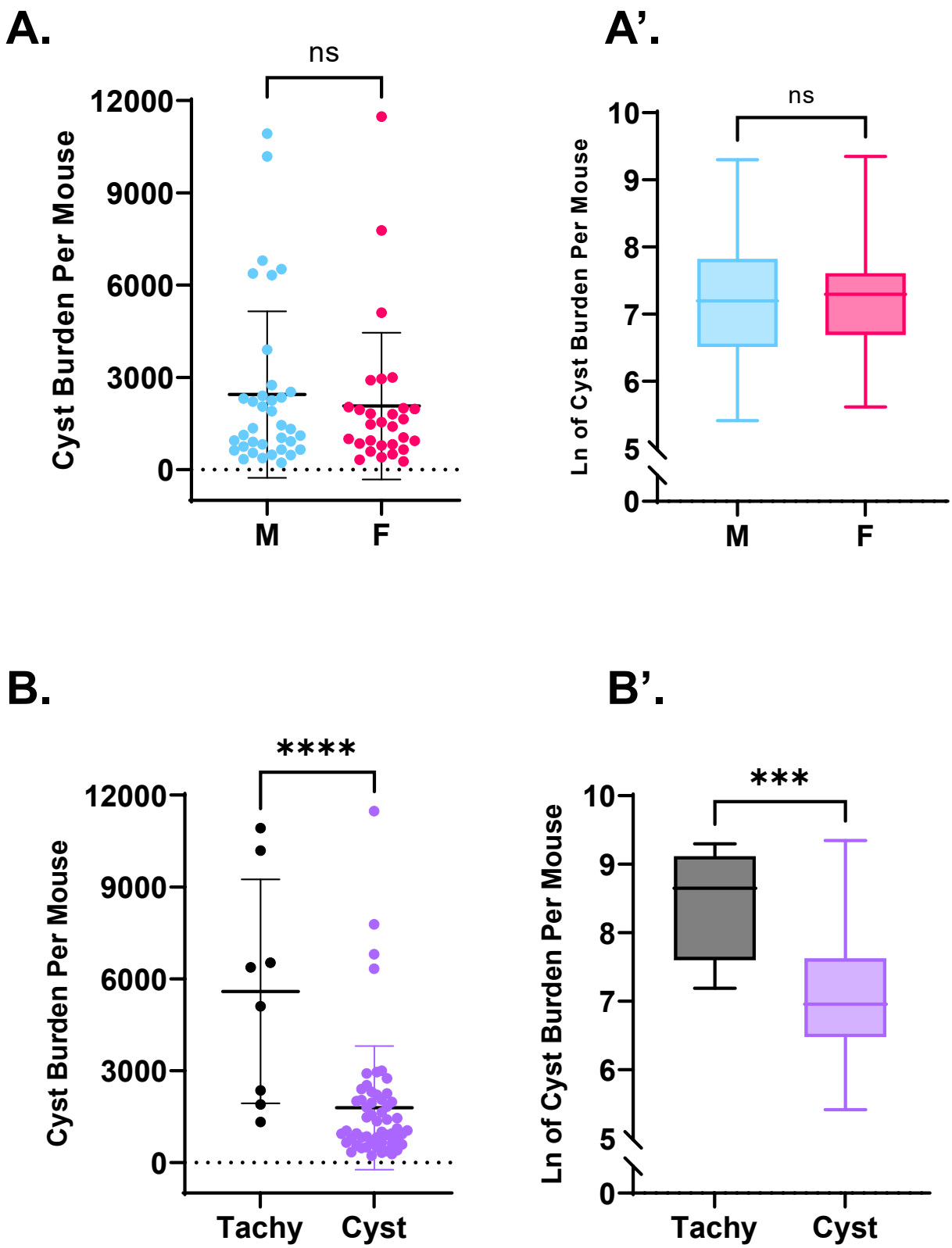

Troublefield et al. 2022 **Figure 5**

A.

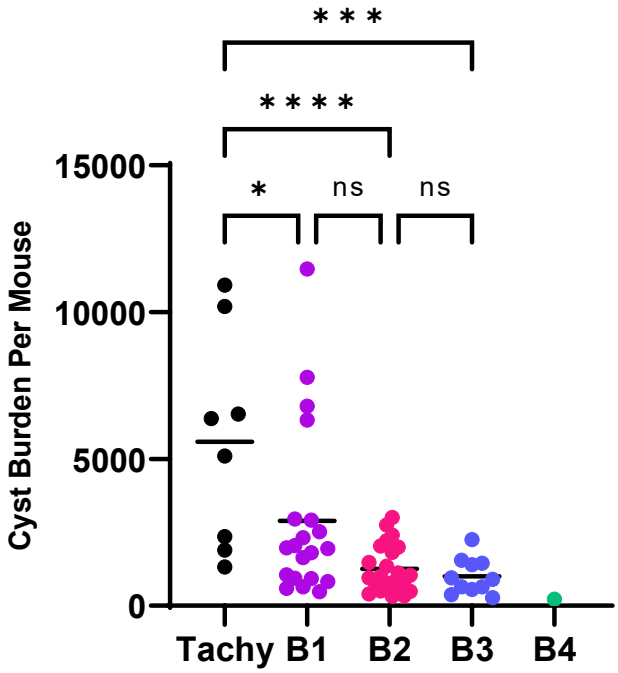

A'.

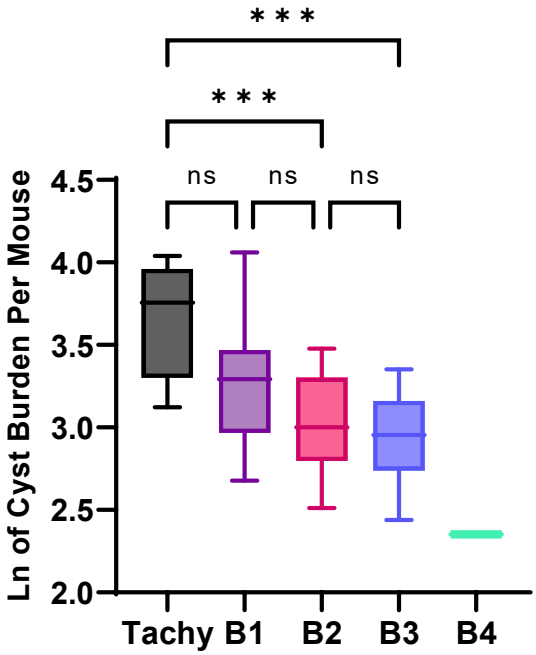

B.

	T	B1	B2	B3	B4
Total mice harvested	16	34	50	28	2
Total mice infected	65	44	62	34	2
Total harvested (%)	24.6%	77.3%	79.4%	82.4%	100%
Mean Cysts per mouse harvested	5091	2863	1178	1040	225
Mean Cysts per mouse infected	1803	2163	931	828	225

Troublefield et al. 2022 **Figure 6**

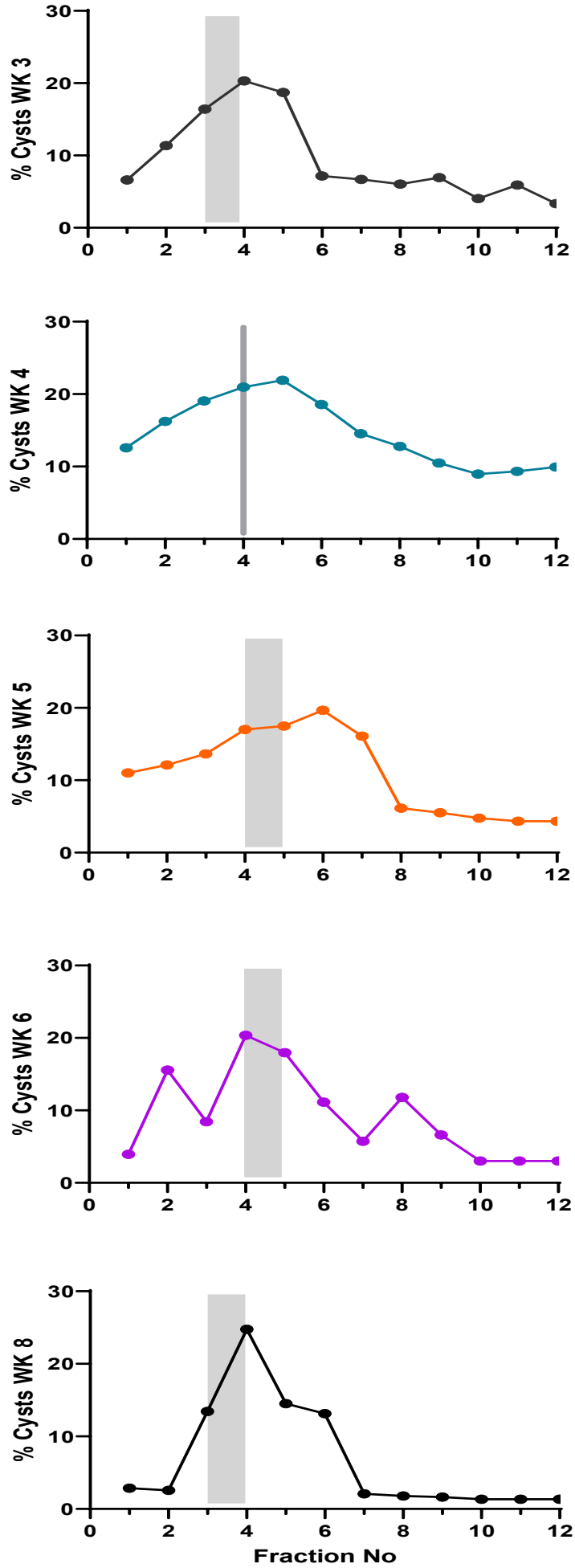

Troublefield et al. 2022 **Figure 7**

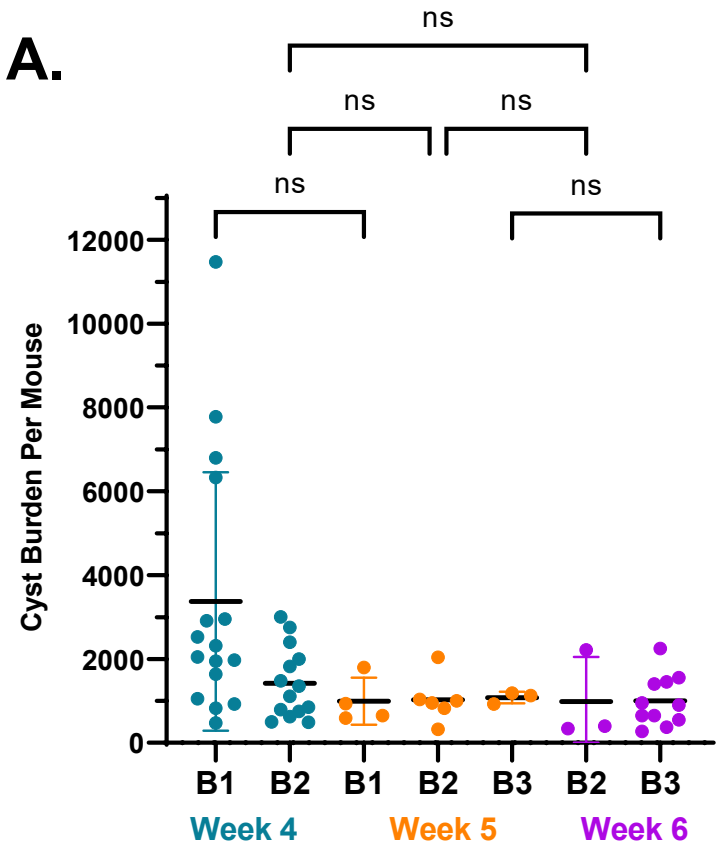

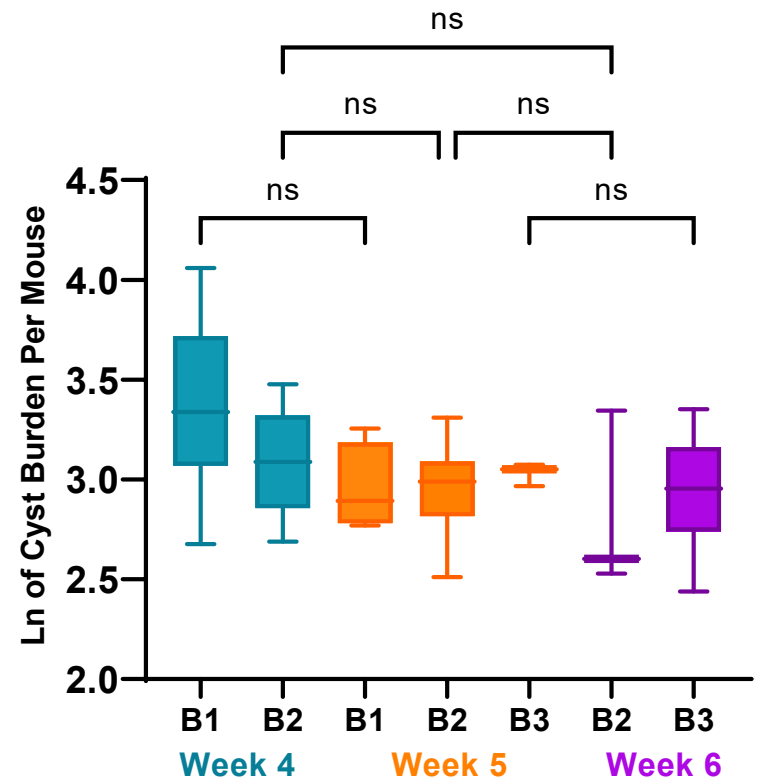

Troublefield et al. 2022 **Figure 8**